



# Extracellular polysaccharides of a bacterium associated with a fungal canker disease of *Eucalyptus* sp

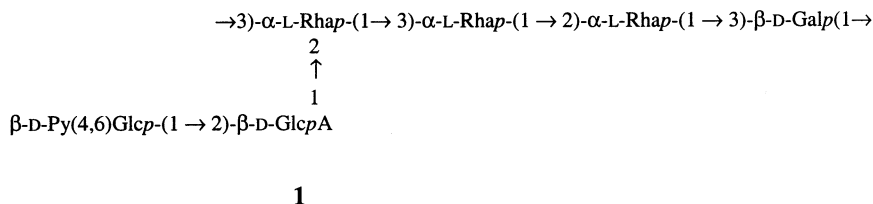
Byung Yun Yang, Qiong Ding, Rex Montgomery\*

*Department of Biochemistry, College of Medicine, University of Iowa, Iowa City, IA 52242, USA*

Received 15 November 2001; accepted 5 February 2002

## Abstract

Extracellular polysaccharides (EPSs) produced by an *Erwinia* sp associated with a fungal canker disease of Eucalyptus were fractionated into one polysaccharide that was identified with that produced by *Erwinia chrysanthemi* strains SR260, Ech1, and Ech9, and the other distinctively different from any other EPS produced by *E. chrysanthemi* strains so far studied. Their structures were determined using a combination of chemical and physical techniques including methylation analysis, low pressure gel-filtration, and anion-exchange chromatographies, high-pH anion-exchange chromatography, mass spectrometry and 1D and 2D  $^1\text{H}$  NMR spectroscopy. The new polysaccharide, identified as EPS Teranera, has the following structure:



The molecular weights of the polysaccharides range from  $3.2\text{--}6.2 \times 10^5$  and their hydrodynamic properties are those of polydisperse, polyanionic biopolymers with pseudoplastic, non-thixotropic flow characteristics in aqueous solutions. © 2002 Elsevier Science Ltd. All rights reserved.

**Keywords:** *Erwinia* spp; Eucalyptus; Extracellular polysaccharide; Structure; Ribotyping

## 1. Introduction

Eucalyptus trees in South Africa are being threatened by a fungal disease that produces cankerous stem lesions that go into the wood, thus damaging it for timber, pulp, and paper uses. The canker is caused by *Coniothyrium zuluense*,<sup>1-3</sup> which is associated with a bacterium that has many properties similar to an *Erwinia* sp. Inoculation of susceptible Eucalyptus with fungus and/or bacterium showed that the fungal isolate can cause the canker without the presence of the bacterium, which cannot produce a canker alone, but the combination of both organisms produced significantly larger lesions than the fungus alone.<sup>3</sup> The present paper reports on the chemotaxonomy and ribotyping of the

**Abbreviations:** EPS, extracellular polysaccharide; EPS6, EPS from Ech6, etc; HPAEC-PAD, high-pH anion-exchange chromatography with pulsed amperometric detection; TFA, trifluoroacetic acid; MALDITOF MS, matrix-assisted laser desorption and ionization time-of-flight mass spectrometry; COSY, correlation spectroscopy; TOCSY, total correlation spectroscopy; NOESY, nuclear Overhauser effect spectroscopy; LS, light scattering;  $\eta$ , viscosity;  $\eta_{sp}$ , specific viscosity;  $\eta_{sp}/c$ , reduced viscosity;  $[\eta]$ , intrinsic viscosity;  $M_w$ , weight-average molecular weight;  $R_w$ , weight-average root mean square radius.

\* Corresponding author. Fax: +1-319-335-9570.

*E-mail address:* [rex-montgomery@uiowa.edu](mailto:rex-montgomery@uiowa.edu) (R. Montgomery).

bacterium, which for the present is identified as *Erwinia teranera*.

## 2. Methods

**Preparation of extracellular polysaccharides.**—The aqueous medium for the preparation of EPS Teranera in Fernbach flasks contained: D-glucose ( $20.0 \text{ g L}^{-1}$ ), proteose peptone ( $2.0 \text{ g L}^{-1}$ ), yeast extract ( $0.5 \text{ g L}^{-1}$ ),  $\text{MgSO}_4 \cdot 7 \text{ H}_2\text{O}$  ( $0.5 \text{ g L}^{-1}$ ), and  $\text{KH}_2\text{PO}_4$  ( $0.5 \text{ g L}^{-1}$ ). Calcium carbonate ( $2.5 \text{ g L}^{-1}$ ) was added after sterilization by autoclaving. A 100 mL quantity of this medium was inoculated with a culture of *E. teranera* grown on nutrient agar. After 3 days, 25 mL of the inoculum was added to 1 L of medium in a Fernbach flask, which was shaken at  $30^\circ\text{C}$  and 150 rpm for the first day, increasing the shaking to 200 rpm for 2 more days. The solution was centrifuged at 14,000 rpm for 2 h or until the supernatant was clear. To the supernatant was added NaCl ( $30 \text{ g L}^{-1}$ ) and the EPS Teranera was precipitated with 2.0–2.5 volumes of EtOH. The crude EPS was dissolved in 5% NaCl, centrifuged and the EPS reprecipitated with EtOH. The yield was  $0.74 \text{ g L}^{-1}$ .

**Purification of polysaccharides by anion-exchange chromatography.**—Crude EPS (80 mg) in water (40 mL) was loaded on the low-pressure anion-exchange column (Toyopearl DEAE-650M,  $2.5 \times 12 \text{ cm}$ ), which had been washed with 100 mL of 1.5 M pyridinium acetate (pH 5.4) and equilibrated with water. The column was washed with water (100 mL), and then irrigated with a linear gradient of pyridinium acetate (300 mL of 1 M pyridinium acetate, pH 5.4 and 300 mL of water) (Fig. 1). The elution was followed by the phenol– $\text{H}_2\text{SO}_4$  method.<sup>4</sup> Fractions containing the car-

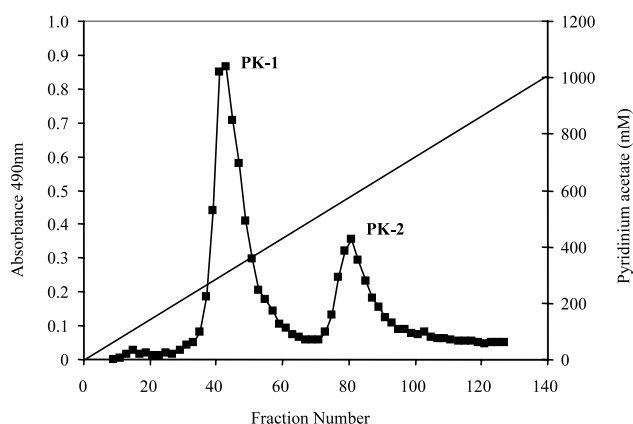


Fig. 1. Anion-exchange chromatographic purification of EPS Teranera on a DEAE650 column ( $2.5 \times 12 \text{ cm}$ ). The column was eluted with a linear gradient of 1 M pyridinium acetate (pH 5.4) and the elution was monitored by the phenol– $\text{H}_2\text{SO}_4$  method.

bohydrate were appropriately pooled and concentrated to dryness in vacuo at  $43^\circ\text{C}$  to give two polysaccharides identified as PK-1 and PK-2.

**Analytical and general methods.**—The methods used for methylation analysis, gas–liquid chromatography with an FID detector (GLC) and mass-selective detector (GC-MS), monosaccharide analysis by high-pH anion-exchange chromatography pulsed amperometric detection (HPAEC-PAD), matrix-assisted laser desorption/ionization time-of-flight mass spectrometric analysis (MALDITOF MS) of per-*O*-methylated derivatives, and 600 MHz  $^1\text{H}$  NMR spectroscopy have been described previously.<sup>5–12</sup>

**Mild-acid hydrolysis of EPS PK-2.**—An aqueous solution of EPS was adjusted to pH 2.1 with 10 mM  $\text{H}_2\text{SO}_4$  and heated at  $120^\circ\text{C}$  for 1 h. The low molecular weight components (filtrate) were separated from the high molecular weight molecules (retentate), using a centrifugal filter (Amicon Centricon, MWCO 3000, Millipore, MA, USA). The retentate was freeze dried and subjected to degradation by lithium in ethylenediamine.<sup>13,14</sup> The filtrate was analyzed for pyruvic acid, which was identified by GC-MS analysis as a trimethylsilyl derivative of 2-deuteriolactic acid as follows: A portion of the filtrate was directly analyzed by high-performance cation-exchange chromatography (HPLC) as described elsewhere.<sup>6,15</sup> The remainder of the filtrate was neutralized with  $\text{NH}_4\text{OH}$  and reduced with  $\text{NaBD}_4$ . Excess of borodeuteride was decomposed with glacial AcOH and the borate removed as the methyl ester by coevaporation with MeOH. The resulting dried material was derivatized as the trimethylsilyl ether and ester.<sup>16–18</sup>

**Isolation of a pyruvated hexasaccharide from EPS PK-2.**—The purified EPS PK-2 (92 mg dried in vacuo at  $80^\circ\text{C}$  for 16 h) in 25 mL screw-capped glass tube was depolymerized using fuming HCl (5 mL of 37.5% HCl, 22 min, rt) as described previously.<sup>6</sup> The resulting clear solution was poured, with stirring, into 100 mL of ice-cold aq NaOAc solution (5.17 g, 63 mmol) in a 250-mL vacuum flask. The resulting solution (pH 3.2) was concentrated to dryness in vacuo at  $43^\circ\text{C}$  by co-evaporation with toluene. The dried residue was mixed with 30 mL of dimethyl sulfoxide ( $\text{Me}_2\text{SO}$ ), and sonicated to produce a slurry. The supernatant was recovered by centrifugation. This step was repeated twice ( $2 \times 10 \text{ mL}$ ). All the supernatants were combined and the oligosaccharides were precipitated by slowly adding  $\text{CHCl}_3$  (250 mL), with stirring, to minimize heat generation. The supernatant, after standing overnight, was decanted and the solids recovered by centrifugation. The residue was washed repeatedly with  $\text{CHCl}_3$  ( $2 \times 20 \text{ mL}$ ), and finally dried in vacuo. The product was redissolved in water (3 mL) and separated on Bio-Gel P-2 and P-4 columns by eluting with 0.1 M pyridinium acetate (pH 5.4) (Fig. 2). The pyruvated

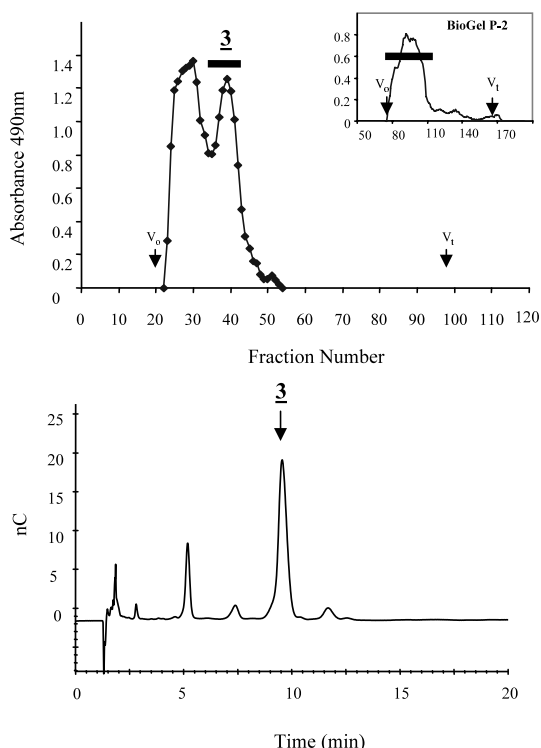


Fig. 2. Gel filtration (top panel) and high-pH anion-exchange (bottom) chromatographic purification of **3** (pyruvated hexasaccharide) from EPS PK-2. Inset in top panel: partial acid hydrolyzates (fuming HCl, 22 min, rt) of EPS PK-2 were fractionated on a BioGel P-2 ( $2.5 \times 85$ , 200–400 mesh) column and the peak under the bar was further fractionated on a BioGel P-4 ( $1.5 \times 84$  cm, 200–400 mesh) column. Purification of the pyruvated hexasaccharide was completed by HPAEC on a semipreparative PA100 column, using isocratic elution by 180 mM NaOAc in the presence of 40 mM NaOH.

hexasaccharide was further purified by HPAEC on a semi-preparative PA100 column ( $9 \times 250$  mm; Dionex Corporation, Sunnyvale, CA), using isocratic elution by 180 mM NaOAc in the presence of 40 mM NaOH. The peak was collected manually and neutralized immediately by addition of glacial AcOH. The oligosaccharide was recovered by lyophilization after removal of  $\text{Na}^+$  on a cation-exchange column (Bio-Rad AG50W-X8,  $\text{H}^+$ ) as described previously.<sup>6–8</sup>

**Analysis of purified EPSs by light scattering (LS).**—EPS was dried to a constant dry weight in a high-vacuum desiccator ( $80^\circ\text{C}$ , 24 h) in order to correct the moisture in subsequent weighing. The carbohydrate concentration was determined by the phenol– $\text{H}_2\text{SO}_4$  method with a monosaccharide composition standard of each EPS.

A series of different concentrations ( $1$ – $5\text{ mg mL}^{-1}$ ) of EPS solution was prepared in  $0.5\text{ M NaCl}$  containing  $0.05\%$   $\text{NaN}_3$ , dialyzed against the same solvent for 3 days, and filtered ( $0.45\text{ }\mu\text{m}$ , Millex-HA, Millipore

Co., Bedford, MA, USA). A portion of filtrate ( $4\text{ mL}$ ) was analyzed with a light scattering detector ( $5\text{ mW}$  linearly polarized He–Ne  $632.8\text{ nm}$  laser, Dawn DSP Laser Photometer, Wyatt Technology Co., Santa Barbara, CA, USA) using a syringe pump at a constant flow rate ( $0.5\text{ mL min}^{-1}$ ). The photometer measures the laser light scattered from the flowing sample at 18 positions, 14 of which were used in this study that ranged from  $38$  to  $141^\circ$ . Data were acquired and analyzed using Wyatt Technology's software (ASTRA V4.72.03) to obtain the molecular weight ( $M_w$ ) and the root mean square radius ( $R_w$ ).

The specific refractive index increment ( $dn/dc$ ) of the EPS was determined with a refractive index detector (ERC-7517 Refractive Index Detector, ERC Inc., Saitama, Japan) at rt. The  $dn/dc$  value was determined from the plot of the refractive index against five different concentrations, ranging from  $1.0$  to  $5.0\text{ mg mL}^{-1}$ , for each EPS. The value of  $dn/dc$  was  $0.155\text{ mL g}^{-1}$  for the EPS PK-1 and  $0.166\text{ mL g}^{-1}$  for the EPS PK-2, and these values did not change in the presence of  $\text{CaCl}_2$ .

**Determination of viscosity.**—The intrinsic viscosity  $[\eta]$  of each EPS solution was measured at  $25^\circ\text{C}$  using Ostwald capillary viscometers and determined by the Huggins and Kraemer plots of relative viscosity and specific viscosity against concentration.<sup>19,20</sup> The effect of ionic strength on the viscosity of the polysaccharide solution was determined by adding a saturated solution of NaCl to the polysaccharide solution. The viscosity of the polysaccharide solutions remained unchanged when the salt concentration reached  $0.3\text{ M}$  or above. All determinations were therefore made in  $0.5\text{ M NaCl}$ .

The viscosity of each EPS solution at different shear rates was determined at  $25^\circ\text{C}$  with a plate-and-cone viscometer (DV-III V3.3 RV, Brookfield Engineering Laboratories Inc., Middleboro, MA, USA).

**Ribotype.**—Ribotyping was performed on a DuPont Qualicon Riboprinter<sup>®</sup> using the procedures outlined by the manufacturer. Picks of bacteria grown overnight on brain–heart Infusion agar were transferred to a sample carrier and heated for 22 min at  $80^\circ\text{C}$  to kill the bacteria. The sample carrier was inserted into the Riboprinter<sup>®</sup>; all subsequent manipulations are automatic and consist of DNA extraction, digestion with EcoRI, electrophoresis and blotting onto a membrane, and probing with a labeled cDNA probe derived from *E. coli* 16S and 23S rRNA. After blotting, the membrane was illuminated and the image was captured with a digital camera. The resulting patterns were analyzed and stored using software supplied by Qualicon. A software program, BIONUMERICS (v 2, Applied Maths, Kortrijk, Belgium), was used for subsequent analysis and plotting of the dendrogram directly from the archived data.

### 3. Results and discussion

The bacterium used in these studies is a Gram-negative, mobile rod and it shows a white growth on nutrient agar containing glucose. The organism shows a low selectivity for *Erwinia chrysanthemi* sp by Vitek and API 20E evaluations (which offer identification systems for Enterobacteriaceae and other Gram-negative rods, BioMerieux, St. Louis, Mo, USA). The organism ferments lactose and does not produce pectate lyase. It does however show a relationship to *Erwinia* sp in that the EPSs include one identical in primary structure to that produced by *E. chrysanthemi* Ech9 and others,<sup>9,10,12</sup> and the second EPS has structural similarities to *E. chrysanthemi* Ech6<sup>11</sup> and A350.<sup>5,7</sup> Tentatively, the bacterium has been designated *E. teranera*.

**Purification and composition analyses of EPS.**—Anion-exchange chromatography of crude EPS resulted in two different acidic EPSs (PK-1 and PK-2), which were present in the approximate ratio of 2:1 (Fig. 1). The EPS PK-1 was eluted at approximately 300 mM pyridinium acetate and the other EPS PK-2 at 600 mM. No neutral oligo- or polysaccharides were present in the EPS preparations.

HPAEC-PAD analysis of the monosaccharide composition (2 M TFA, 120 °C, 1 h) revealed that each EPS

is homogeneous, as determined by constant composition across the anion-exchange chromatography peak. EPS PK-1 has the composition of L-Rha, D-Glc, D-Man, and D-GlcA in the ratio 3:1:1:1 and EPS PK-2 that of L-Rha, D-Glc, D-Gal, and D-GlcA in the ratio 3:1:1:1. The presence of GlcA residues in these EPSs was confirmed by HPAEC-PAD analyses of monosaccharide composition of carboxyl-reduced EPS.<sup>21–23</sup> The absolute configurations of the sugar residues were determined as the TMS derivatives of the R-(–)-butan-2-ol glycosides by GLC analysis.<sup>24</sup>

***Teranera* EPS PK-1.**—Glycosyl linkage-analysis of the EPS PK-1 after reduction of the per-*O*-methylated EPS with Super-Deuteride (to convert the GlcA to Glc), showed the presence of one residue of terminal Rha, two residues of 3-linked Rha and one residue each of 3,4-linked Man, 3-linked Glc and 4-linked GlcA (Table 1). It is evident from the glycosyl linkage analysis that the EPS has a branched hexasaccharide repeating unit. The extremely likelihood based on the precedence of mannosyl and glucosyluronic residues being in the pyranose ring form, all of the residues in the EPS are present in the pyranose form.

The presence of a hexasaccharide repeat-unit in the native EPS is confirmed by the presence of six anomeric protons in the 1D <sup>1</sup>H NMR spectrum (Fig. 3 and Table

Table 1  
Glycosyl linkage-analyses of native and backbone EPSs and reduced pyruvated hexasaccharide from *E. teranera*

Me sugar <sup>d</sup>	PK-1		PK-2			
	Native <sup>a</sup>	Backbone <sup>a</sup>	Native <sup>a</sup>	de-EPS <sup>b</sup>	Backbone <sup>a</sup>	3 <sup>c</sup>
1,2,4,5,6-Me <sub>5</sub> Gal						0.4
2,3,4-Me <sub>3</sub> Rha	0.8					
3,4-Me <sub>2</sub> Rha			0.9	0.9	1.0	2.0
2,4-Me <sub>2</sub> Rha	2.1	1.0	1.0	1.0	2.0	1.1
2,3,4,6-Me <sub>4</sub> Glc				0.6		
4-MeRha			1.1	0.9		
2,4,6-Me <sub>3</sub> Gal			1.0	0.8	1.0	
2,4,6-Me <sub>3</sub> Glc	1.0	0.8				
2,3-Me <sub>2</sub> Glc <sup>e</sup>			1.1			1.0
2,6-Me <sub>2</sub> Man	1.0					
2,3,6-Me <sub>3</sub> Man		1.0				
2,3-Me <sub>2</sub> GlcA <sup>f</sup>	1.0					
3,4-Me <sub>2</sub> GlcA <sup>f</sup>			0.7	0.4		0.8
2,3,4-Me <sub>3</sub> GlcA <sup>f</sup>				0.3		

<sup>a</sup> Before and after Li-treatment, respectively.

<sup>b</sup> PK-2 EPS heated at pH 2.1 and 120 °C for 1 h. De-pyruvated EPS recovered as retentate of Centricon (3000 MWCO).

<sup>c</sup> Pyruvated hexasaccharide isolated from partial acid (fuming HCl, 22 min) hydrolyzates of PK-2 EPS and then reduced with NaBH<sub>4</sub>. The resulting oligosaccharide alditol was methylated.

<sup>d</sup> 2,4-Me<sub>2</sub>Rha = 1,3,5-tri-*O*-acetyl-1-deuterio-2,4-di-*O*-methyl Rha-ol.

<sup>e</sup> Derived from 4,6-*O*-(1-carboxyethylidene)-Glc.

<sup>f</sup> Observed as 1,4,5,6-tetra-*O*-acetyl-1,6,6-trideuterio-2,3-di-*O*-methyl Glc-ol derived from the reduction of the methyl ester of 2,3-Me<sub>2</sub>GlcA with Super-Deuteride and etc.

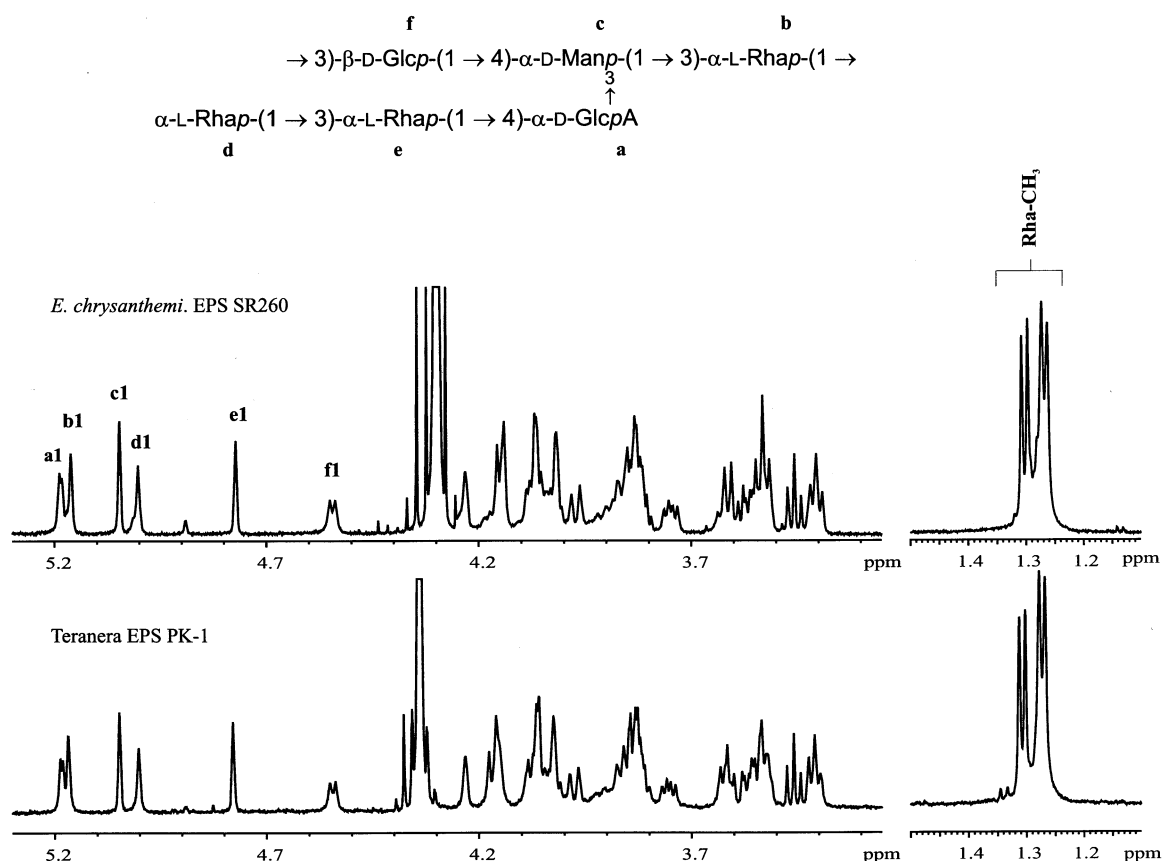


Fig. 3. The 600 MHz 1D  $^1\text{H}$  NMR spectra of EPS PK-1 and EPS SR260 recorded in  $\text{D}_2\text{O}$  containing 1% NaCl at 65 °C.

Table 2

NMR data for Teranera EPS TPK-1 and EPS SR 260

	Residue of inferred linkage in the native EPS	$\delta_{\text{H}}$ (ppm) <sup>a</sup>	
		EPS PK-1	EPS SR260 <sup>b</sup>
a	$\rightarrow 4\text{-}\alpha\text{-D-GlcpA}\text{-}(1 \rightarrow$	5.184	5.185
b	$\rightarrow 3\text{-}\alpha\text{-L-Rhap}\text{-}(1 \rightarrow$	5.168	5.162
c	$\rightarrow 3,4\text{-}\alpha\text{-D-Manp}\text{-}(1 \rightarrow$	5.048	5.047
d	$\alpha\text{-L-Rhap}\text{-}(1 \rightarrow$	5.002	5.003
e	$\rightarrow 3\text{-}\alpha\text{-L-Rhap}\text{-}(1 \rightarrow$	4.780	4.772
f	$\rightarrow 3\text{-}\beta\text{-D-Glcp}\text{-}(1 \rightarrow$	4.545	4.544

The spectra were obtained in  $\text{D}_2\text{O}$  containing 1% NaCl, 65 °C.

<sup>a</sup> Chemical shifts relative to acetone ( $\delta_{\text{H}}$  2.225 ppm).

<sup>b</sup> Refs. 9, 10, and 12.

2). The chemical shifts and coupling constants indicate that the resonances at  $\delta$  5.184 ppm ( $J_{1,2}$  3.7 Hz, 1 H) and at  $\delta$  4.545 ppm ( $J_{1,2}$  7.7 Hz, 1 H) are characteristic of the  $\alpha$ - and  $\beta$ -gluco configuration, which were arising from a GlcA residue and Glc, respectively. The four signals with unresolved coupling constants at  $\delta$  5.168, 5.048, 5.002, and 4.780 ppm, arise from three Rha and one Man residues of  $\alpha$ -manno configuration, identical to those of EPS produced by *E. chrysanthemi* strains

SR260, Ech1, and Ech9.<sup>5,9,10,12</sup> Nine protons (three doublets) corresponding to the three 6-deoxy groups of Rha, were observed at  $\delta$  1.308 ( $J_{5,6}$  6.2 Hz), 1.273 ( $J_{5,6}$  6.2 Hz), and 1.273 ( $J_{5,6}$  6.2 Hz) ppm.

Degradation of the EPS PK-1 by lithium, where glycosyluronic residue is cleaved and the released sugar is reduced, generated a modified EPS and low molecular weight components from fractionation on BioGel P-2 (data not shown). The low molecular weight com-



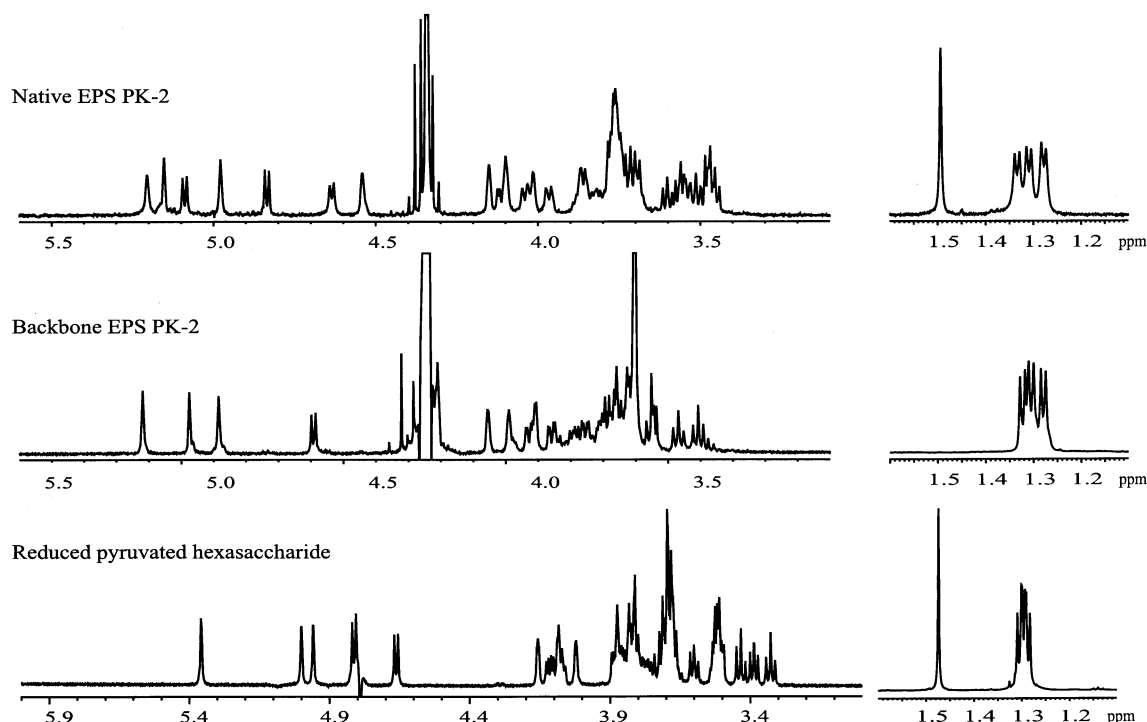


Fig. 5. The 600 MHz 1D  $^1\text{H}$  NMR spectra of native EPS PK-1 (top panel), backbone (middle), and reduced compound 3 (bottom). The spectra obtained of the EPS in  $\text{D}_2\text{O}$  containing 1% NaCl at 65  $^\circ\text{C}$  and reduced compound 3 at 25  $^\circ\text{C}$ , pD 6.5. The HOD peak was suppressed in the NMR spectrum of reduced compound 3 but not the other NMR spectra.

GlcA and terminal Glc. The presence of pyruvate in the EPS was identified by HPLC analysis<sup>6,15</sup> of pyruvate released from the native EPS by mild-acid hydrolysis (pH 2.1, 120  $^\circ\text{C}$ , 1 h). Under such conditions, pyruvic acid was completely cleaved from the EPS as detected, in the methylation analysis, by the complete loss of 1,4,5,6-tetra-*O*-acetyl-1-deuterio-2,3-di-*O*-methyl Glc-ol in the per-*O*-methylated EPS and the appearance of 1,5-di-*O*-acetyl-1-deuterio-2,3,4,6-tetra-*O*-methyl Glc-ol (Table 1). Significant amounts of glycosyl cleavage of the terminal Glc residue also occurred as observed in the low recovery of the terminal Glc residue by glycosyl linkage analysis compared with the native EPS, which consequently generated a new terminal GlcA residue (as detected by 1,5,6-tri-*O*-Ac-1,6,6-tri-deuterio-2,3,4-*O*-tri-methyl Glc-ol).

The evidence of a hexasaccharide repeating-unit in the native EPS TPK2 was supported by the presence of six anomeric protons in the 1D  $^1\text{H}$  NMR spectrum (Fig. 5). The chemical shifts and coupling constants indicate that the three resonances at  $\delta$  5.205 ppm ( $J_{1,2}$  unresolved, 1 H),  $\delta$  5.152 ppm ( $J_{1,2}$  unresolved, 1 H) and  $\delta$  4.978 ppm ( $J_{1,2}$  unresolved, 1 H) are characteristic of an  $\alpha$ - and  $\beta$ -manno configuration, arising from each anomeric proton of three Rha residues. The three signals at  $\delta$  5.089 ppm ( $J_{1,2}$  7.8 Hz, 1 H),  $\delta$  4.835 ppm ( $J_{1,2}$  7.8 Hz, 1 H) ppm, and  $\delta$  4.635 ppm ( $J_{1,2}$  7.1 Hz, 1 H) are characteristic of a  $\beta$ -gluco or galacto configura-

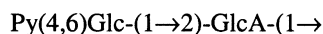
tion, thus arising from each anomeric proton of Glc, Gal, and GlcA residues. The resonance at  $\delta$  5.089 ppm is significantly downfield shifted for the typical anomeric protons of  $\beta$ -hexosyl residues, but such an unusual chemical shift has been observed with 2-substituted  $\beta$ -Glc<sub>p</sub> residue in other lipopolysaccharide of *Moraxella catarrhalis* serotype B (strain CCUG 3292) or derived oligosaccharides<sup>29</sup>.

Nine protons of three doublets corresponding to the three methyl groups of Rha, were observed at  $\delta$  1.334 ( $J_{5,6}$  5.7 Hz), 1.309 ( $J_{5,6}$  5.8 Hz) and 1.278 ( $J_{5,6}$  5.7 Hz) ppm. The 1D  $^1\text{H}$  NMR spectrum also revealed that the methyl group of pyruvate observed at 1.493 ppm, quantitatively capped the Glc residue.

In preparation for lithium degradation of the EPS, it was found that the native EPS PK-2 was not soluble in ethylenediamine until the pyruvate was removed. The depyruvated EPS PK-2 was degraded by lithium in ethylenediamine. Two fragments of high- and low-molecular weights were fractionated on a BioGel P-2 column (data not shown). The low-molecular weight components run with salt on the column, thus recovered by acetylation using  $\text{Ac}_2\text{O}$  in pyridine. It comprised mainly of Glc-ol, determined by GLC analysis of the resulting derivative. The high-molecular weight fraction was composed of Gal and Rha in a 1:3 molar ratio and by glycosyl-linkage analysis there were 3-linked Gal, 3-linked Rha, and 2-linked Rha residues in a 1:2:1 molar ratio. The backbone EPS in 1D  $^1\text{H}$  NMR

spectrum (Fig. 5) had three Rha resonances with unresolved coupling constants at  $\delta$  5.219 ppm ( $J_{1,2}$  unresolved, 1 H),  $\delta$  5.075 ( $J_{1,2}$  unresolved, 1 H), and  $\delta$  4.985 ( $J_{1,2}$  unresolved, 1 H), and one  $\beta$ -Gal signal at  $\delta$  4.693 ( $J_{1,2}$  7.8, 1 H). The three doublets at  $\delta$  1.323 ppm ( $J_{5,6}$  6.0 Hz),  $\delta$  1.305 ppm ( $J_{5,6}$  6.0 Hz), and  $\delta$  1.280 ppm ( $J_{5,6}$  6.0 Hz) were also present, corresponding to the 6-deoxy groups of three Rha residues. Moreover, the retention of one  $\beta$ -anomeric signal and the losses of two  $\beta$ -anomeric signals in the EPS backbone support the side chain comprising  $\beta$ -D-Glc and  $\beta$ -D-GlcA in the native EPS. Therefore, the backbone has a tetrasaccharide repeating subunit consisting of three Rha and one Gal residues, which is consistent with methylation data described above.

It was evident from the glycosyl linkage analysis and the other data that all of the residues in the EPS are in the pyranose form, that the EPS has a branched pyruvated hexasaccharide repeating unit, and that pyruvated glucosylglucosyluronic residue (**2**) is in the side chain.



**2**

The backbone of the native EPS consists of a linear tetrasaccharide repeat subunit that is substituted by the side chain **2** at O-2 of a branch point Rha residue in the native EPS.

The pyruvated hexasaccharide **3** isolated from the depolymerized EPS by fuming HCl had a monosaccharide composition of three Rha residues and one residue each of Glc, GlcA, and Gal by HPAEC-PAD analysis, identical to that of the native EPS. The per-*O*-methylated derivative of **3** by MALDITOF MS was found to have a mass of  $m/z$  1273.2, which is in good agreement with the calculated sodium adduct ( $m/z$  1273.4) for a pyruvated hexasaccharide subunit of the EPS. Methylation analysis of pre-reduced **3** (with NaBH<sub>4</sub>) revealed that it contained Gal at the reducing end and pyruvated Glc residue at the nonreducing end, but no branching residue was detected (Table 1). It also contained one extra mole of 2-linked Rha residue on the expense of the 2,3-linked Rha residue in the native EPS. Consequently this linear and Gal terminating hexasaccharide establishes that both the side chain **2** and Gal residue are linked to the branching Rha residue in the native EPS, at O-2 and O-3, respectively. The low recovery of the reduced-reducing terminal residue is due to the volatility of 3-*O*-acetyl-1,2,4,5,6-penta-*O*-methyl Gal-ol under the experimental conditions.

The 600 MHz 1D <sup>1</sup>H NMR spectrum obtained of pre-reduced **3** (3 mM sodium salts, pD 6.5, 25 °C) had the signals of the five anomeric protons in stoichiometric ratio, of which three Rha residues are present in the  $\alpha$  configuration (discussed later), and both Glc and GlcA

residues in the  $\beta$  configuration (Fig. 5). The 1D <sup>1</sup>H NMR spectrum also revealed that three doublets ( $J_{5,6}$  6.0 Hz) corresponding to methyl groups of three Rha residues were present at  $\delta$  1.296, 1.304, and 1.288 ppm. The methyl group of pyruvate was also observed at  $\delta$  1.474 ppm and quantitatively capped to the nonreducing terminal Glc residue as determined by the area ratio (1.0:3.1) of anomeric proton to methyl protons. The chemical shift of the methyl group of the pyruvic acid indicates an equatorial conformation of the methyl group, accordingly the *S* configuration to the pyruvic acid substituent.<sup>30</sup>

Assignments of the spin systems of the glycosyl residues in pre-reduced **3** were completed by the combination of two-dimensional (<sup>1</sup>H, <sup>1</sup>H) correlation spectroscopy (COSY), total correlation spectroscopy (TOCSY), and nuclear Overhauser effect spectroscopy (NOESY) (Fig. 6).

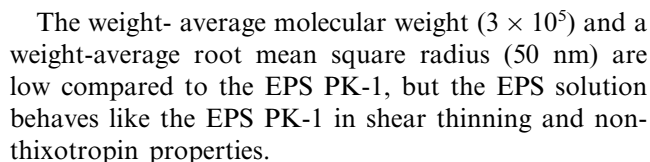
Each Rha residue can be assigned from the characteristic spin system of the small coupling constants between H-2 and H-1 (1.2 Hz) and between H-2 and H-3 (3–4 Hz). A cross-peak relationship from the COSY experiment leads to complete the assignments of H-3, H-4, and H-5, where H-5 showed a cross-peak to H-6. The  $\beta$ -configured Glc and GlcA residues were characterized by large coupling constants due to the trans diaxial relationship of vicinal protons.

The complete spin system of each glycosyl residue from H-1 to H-5 or H-6 was detected in the TOCSY experiment. This permitted the complete assignments of proton resonances of each residue with the cross peak of each spin system from the COSY spectrum. The coupling constants were extracted from 1D NMR spectrum of Gaussian resolution enhancement (data matrix multiplied by Gaussian function prior to Fourier transformation) and the results are summarized in Table 4. The spin system of the reduced terminal residue, Gal-ol was assigned with aid of the NOE contacts of the Gal-ol residue from H-1 of the proximal Rha residue (residue B in Fig. 6), as observed at 3.84, 3.81, and 3.68. These peaks enabled the spin system of the Gal-ol residue to be assigned, along with the COSY and TOCSY experiments.

In the NOESY spectrum there was clear inter-residue connective signals, as well as intra-residue cross peaks (Table 5). In the three Rha residues (A, B, and C) the lack of intra-residue connectivities both between H-1 and H-3, and between H-1 and H-5 is consistent with the  $\alpha$  configuration. The C, D, and E residues had one NOE contact each between two residues: C-1–B-2, D-1–E-2, and E-1–A-2. Thus the sequence of D–E–A and C–B can be unambiguously established. There were two inter-residue NOE contacts, A-1–C-2 (weak signal) and A-1–C-3 (strong signal) and methylation analysis was used to assign the linkage of A-1–C-3.



The addition of calcium ions increases the intrinsic viscosity of the EPS solution as observed in the EPS PK-1 solution, but the properties of the two EPS are



different at a low concentration of calcium added. The  $[\eta]$  of the EPS PK-2 remains unchanged with an increase in calcium, where the first additions of calcium ions are associated with carboxylate groups of the

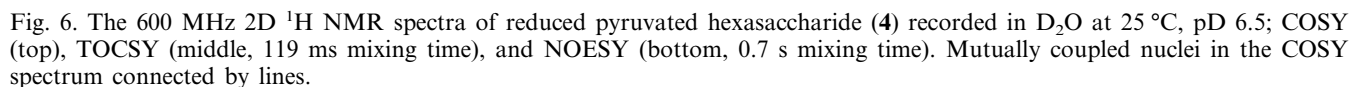


Table 4

<sup>1</sup>H NMR chemical shifts and coupling constants for the reduced pyruvated hexasaccharide in D<sub>2</sub>O at 25 °C and pD 6.5

Residue of inferred linkage		$\delta^a$ (ppm)/ $^3J_{\text{H/H}}$ (Hz)						
		H-1	H-2	H-3	H-4	H-5	H-6	H-6'
a	→2)-α-L-Rhap-(1 →	5.358	4.086	3.834	3.328	3.832	1.296	
		1.2	3.6	10.2	9.6	6.0		
b	→2)-α-L-Rhap-(1 →	5.001	4.023	3.885	3.523	3.791	1.304	
		1.2	3.0	10.2	9.6	6.0		
c	→3)-α-L-Rhap-(1 →	4.960	4.158	3.866	3.509	3.775	1.288	
		1.8	3.6	9.6	9.6	6.0		
d	β-D-Py(4,6) Glcp <sup>b</sup> -(1 →	4.814	3.388	3.691	3.434	3.532	4.116	3.709
		7.8	8.4	9.0	9.6	10.2	13.2	
e	→2)-β-D-GlcpA-(1 →	4.664	3.601	3.694	3.504	3.706		
		7.8	9.0	9.6	9.6			
	→3)-D-Gal-ol	3.84 (1 H), 3.81 (2 H), 3.68 (2 H), and 3.67 (1 H) observed, not determined completely						

<sup>a</sup> Relative to the internal signal of acetone ( $\delta$  2.225 ppm).<sup>b</sup> CH<sub>3</sub> of pyruvic acid observed as a singlet at  $\delta$  1.474.

Table 5

NOE data for the reduced pyruvated hexasaccharide

Residue		Anomeric proton (H-1)	Connectivity residue and chemical shifts	
		$\delta$ (ppm)		$\delta$ H (ppm)
a	→2)-α-L-Rhap-(1 →	5.358	A-1–A-2	4.086
			A-1–C-2	4.158
			A-1–C-3	3.866
b	→2)-α-L-Rhap-(1 →	5.001	B-1–B-2	4.023
			B-1–Gal <sub>ol</sub>	3.791
				3.833
				3.812
c	→3)-α-L-Rhap-(1 →	4.960	C-1–C-2	4.158
			C-1–B-2	4.023
d	β-D-Py(4,6) Glcp-(1 →	4.814	D-1–D-2	3.388
			D-1–D-3	3.691
			D-1–D-5	3.532
			D-1–E-2	3.601
e	→2)-β-D-GlcpA-(1 →	4.664	E-1–E-2	3.601
			E-1–E-3	3.694
			E-1–E-5	3.706
			E-1–A-2	4.086

The spectra were recorded in D<sub>2</sub>O at 25 °C, pD 6.5 and 0.7 s mixing time.

pyruvate and glucuronic acid residues on the same chain with little influence on the  $[\eta]$ .

Fuming HCl has been used for limited non-specific depolymerization of polysaccharides,<sup>31</sup> where the rates of hydrolysis of different glycosidic linkages do not differ significantly. In this study, fuming HCl reacted differently in that a three-substituted β-Galp residue was preferentially cleaved over 6-deoxy hexosyl linkage. A similar effect was also observed with previous works for oligosaccharide preparations from other polysac-

charides *E. chrysanthemi* A350<sup>7</sup> and *Erwinia stewartii* strain DC 283,<sup>32</sup> in which a three-substituted β-Galp residue was present as a proximal residue to the branching point as in this polysaccharide. Thus fuming HCl seems to have some hydrolytic selectivity on that linkage.

**Taxonomical implication.**—The bacterium, designated here as *E. teranera*, isolated from Teranera in the southern parts of Kwazulu-Natal, South Africa, is not of the *E. chrysanthemi* family but produces EPS with

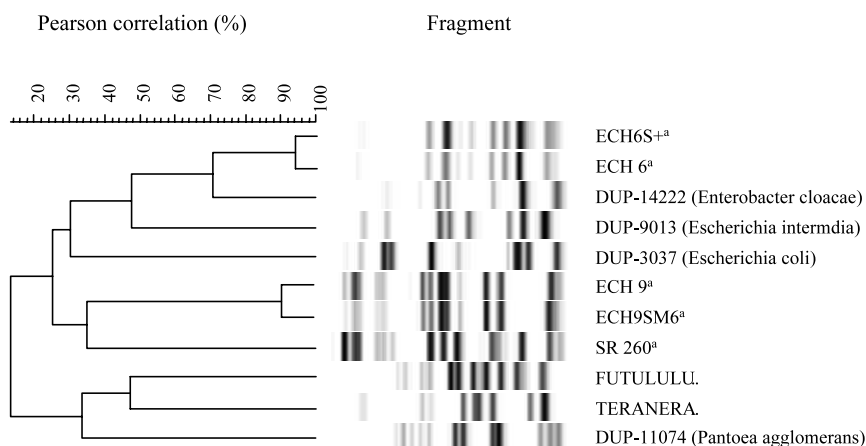


Fig. 7. Nearest-neighbor analysis of the ribotyping data from the *E. chrysanthemi* strains used in this study. <sup>a</sup> Ref. 5.

repeating-unit structures like those of that species. It had been proposed that the EPS of *E. chrysanthemi* sp could be grouped into four families according to their structure and that the ribotyping of the bacteria followed the same grouping.<sup>5,7</sup> It is now clear that this chemotaxonomy and ribotyping are not consistent. The one EPS from *E. teranera* has a repeating-unit structure identical with that from *E. chrysanthemi* Ech9, although the physical properties, size, and viscosity differ. The second EPS from *E. teranera* has the repeating-subunit structure of the backbone similar to that from *E. chrysanthemi* A350, and a pyruvated unit structure similar to that from *E. chrysanthemi* Ech6, a species that is atypical in that it produces no pectate lyase, in contrast to other *E. chrysanthemi*; neither does *E. teranera* produce pectate lyase. The ribotyping of *E. teranera* shows distinct differences from these two strains (Fig. 7), which also excludes the possibility of accidental cross contamination.

### Acknowledgements

The authors thank the Biotechnology Byproducts Consortium (USDA Grant No. 98-34188-5902) and the Carbohydrate Structure Facility for the use of its equipment. We also wish to thank Dr T.A. Coutinho and Dr L.M. VanZyl, Forestry and Agricultural Biotechnology Institute, University of Pretoria, South Africa for the bacterial cultures, Dr James S.S. Gray for many discussions, John Snyder for recording the <sup>1</sup>H NMR spectra, Richard J. Hollis for the ribotyping and Carol Yang for the clinical microbiological characterizations.

### References

1. Wingfield, M. J.; Crous, P. W.; Coutinho, T. A. *Mycopathologia* **1996–1997**, *136*, 139–145.
2. Van Zyl, L. M. In *Ph.D. Thesis*. Factors Associated with Coniothyrium Canker of Eucalyptus in South Africa; University of the Orange Free State, 1999; p. 193.
3. Van Zyl, L. M.; Coutinho, T. A.; Wingfield, M. J.; Pongpanich, K.; Wingfield, B. D. *Mycolog. Res.* **2001**, in press.
4. Dubois, M.; Gilles, K. A.; Hamilton, J. K.; Roberts, P. A.; Smith, F. *Anal. Chem.* **1956**, *28*, 350–356.
5. Yang, B. Y.; Brand, J. M.; James, J. S. S.; Montgomery, R. *Carbohydr. Res.* **2001**, *333*, 295–302.
6. Yang, B. Y.; Brand, J.; Montgomery, R. *Carbohydr. Res.* **2001**, *331*, 59–67.
7. Gray, J. S. S.; Yang, B. Y.; Montgomery, R. *Carbohydr. Res.* **2000**, *324*, 255–267.
8. Yang, B. Y.; Gray, J. S.; Montgomery, R. *Carbohydr. Res.* **1999**, *316*, 138–154.
9. Yang, B. Y.; Gray, J. S. S.; Montgomery, R. *Int. J. Biol. Macromol.* **1996**, *19*, 223–226.
10. Gray, J. S. S.; Koerner, T. A. W.; Montgomery, R. *Carbohydr. Res.* **1995**, *266*, 153–159.
11. Yang, B. Y.; Gray, J. S. S.; Montgomery, R. *Int. J. Biol. Macromol.* **1994**, *16*, 306–312.
12. Gray, J. S. S.; Brand, J. M.; Koerner, T. A. W.; Montgomery, R. *Carbohydr. Res.* **1993**, *245*, 271–287.
13. Lau, J. M.; McNeil, M.; Darvill, A. G.; Albersheim, P. *Carbohydr. Res.* **1987**, *168*, 219–243.
14. Lau, J. M.; McNeil, M.; Darvill, A. G.; Albersheim, P. *Carbohydr. Res.* **1987**, *168*, 245–274.
15. Yang, B. Y.; Montgomery, R. *Carbohydr. Res.* **2000**, *323*, 156–162.
16. Yang, B. Y.; Montgomery, R. *Carbohydr. Res.* **1996**, *280*, 27–45.
17. Gates, S. G.; Dendramis, N.; Sweely, C. C. *Clin. Chem.* **1978**, *24/10*, 1674–1679.
18. Peterson, G. *Carbohydr. Res.* **1974**, *33*, 47–61.
19. Huggins, M. L. *J. Am. Chem. Soc.* **1942**, *64*, 2716–2718.
20. Kraemer, E. O. *Ind. Eng. Chem.* **1938**, *30*, 1200–1203.
21. Karamanos, N. K.; Hjerpe, A.; Tseggenidis, T. *Anal. Biochem.* **1988**, *172*, 410–419.
22. Taylor, R. L.; Conrad, H. E. *Biochemistry* **1972**, *11*, 1383–1388.
23. Hoare, D. D.; Koshland, D. E., Jr. *J. Biol. Chem.* **1967**, *242*, 2447–2453.
24. Gerwig, G. J.; Kamerling, J. P.; Vliegthart, J. F. G. *Carbohydr. Res.* **1978**, *62*, 349–357.
25. Zimm, B. J. *J. Chem. Phys.* **1948**, *16*, 1093–1099.

26. Oba, T.; Higashimura, M.; Iwasaki, T.; Matser, A. M.; Steenken, P. A. M.; Robijn, G. W.; Sikkema, J. *Carbohydr. Polym.* **1999**, *39*, 275–281.
27. Gianni, R.; Cescutti, P.; Bosco, M.; Fett, W. F.; Rizzo, R. *Int. J. Biol. Macromol.* **1999**, *26*, 249–253.
28. Bozzi, L.; Milas, M.; Rinaudo, M. *Int. J. Biol. Macromol.* **1996**, *18*, 83–91.
29. Edebrink, P.; Jansson, P.-E.; Widmalm, G.; Holme, T.; Rahman, M. *Carbohydr. Res.* **1996**, *295*, 127–146.
30. Jansson, P.-E.; Lindberg, J.; Widmalm, G. *Acta Chem. Scand.* **1993**, *47*, 711–715.
31. Jansson, P.-E.; Widmalm, G. *Carbohydr. Res.* **1992**, *231*, 325–328.
32. Yang, B. Y.; Gray, J. S.; Montgomery, R. *Carbohydr. Res.* **1996**, *296*, 183–201.